Chemistry & Biology, Vol. 9, 1109–1118, October, 2002, ©2002 Elsevier Science Ltd. All rights reserved. PII S1074-5521(02)00237-5

Multisite and Multivalent Binding between Cyanovirin-N and Branched Oligomannosides: Calorimetric and NMR Characterization

Shilpa R. Shenoy,[1] Laura G. Barrientos,[2] Daniel M. Ratner,[3] Barry R. O'Keefe,[1] Peter H. Seeberger,[3] Angela M. Gronenborn,[2,5] and Michael R. Boyd[4,5]

[1]Molecular Targets Discovery Program
NCI Center for Cancer Research
National Cancer Institute, NCI-Frederick
Frederick, Maryland 21702

[2]Laboratory of Chemical Physics
National Institute of Diabetes
and Digestive and Kidney Diseases
National Institutes of Health
Bethesda, Maryland 20892

[3]Department of Chemistry
Massachusetts Institute of Technology
Cambridge, Massachusetts 02139

[4]USA Cancer Research Institute
College of Medicine
University of South Alabama
Mobile, Alabama 36688

Summary

Binding of the protein cyanovirin-N to oligomannose-8 and oligomannose-9 of gp120 is crucially involved in its potent virucidal activity against the human immunodeficiency virus (HIV). The interaction between cyanovirin-N and these oligosaccharides has not been thoroughly characterized due to aggregation of the oligosaccharide-protein complexes. Here, cyanovirin-N's interaction with a nonamannoside, a structural analog of oligomannose-9, has been studied by nuclear magnetic resonance and isothermal titration calorimetry. The nonamannoside interacts with cyanovirin-N in a multivalent fashion, resulting in tight complexes with an average 1:1 stoichiometry. Like the nonamannoside, an α1→2-linked trimannoside substructure interacts with cyanovirin-N at two distinct protein subsites. The chitobiose and internal core trimannoside substructures of oligomannose-9 are not recognized by cyanovirin-N, and binding of the core hexamannoside occurs at only one of the sites on the protein. This is the first detailed analysis of a biologically relevant interaction between cyanovirin-N and high-mannose oligosaccharides of HIV-1 gp120.

Introduction

Entry of the human immunodeficiency virus (HIV) into host cells is critically dependent on interactions between the viral envelope glycoproteins (gp120 and gp41) and cellular receptor proteins (CD4, CCR5, and CXCR4). The envelope glycoprotein gp120 of HIV is heavily glycosylated [1], and of the 24 potential *N*-linked glycosylation sites on gp120, eleven are occupied by high-mannose oligosaccharides [2]. These high-mannose oligosaccharides appear to play a protective role for the virus, shielding highly conserved protein domains of gp120 from proteolytic attack and/or the host immune system [3]. Therapeutic targeting of high-mannose oligosaccharides near or within the conserved amino acid regions of gp120 presents a unique opportunity for the development of broadly neutralizing antiviral drugs.

Cyanovirin-N (CV-N), an 11 kDa protein originally purified from an extract of the cyanobacterium *Nostoc ellipsosporum* [4], binds potently to high-mannose oligosaccharides [5] on gp120 and gp41 and in this manner is able to inactivate a broad spectrum of HIV-1, HIV-2, and simian immunodeficiency virus (SIV) strains [4]. The inhibitory activity of CV-N against HIV is at least 1000-fold higher (EC_{50} = 1 ng/ml; [4]) than the reported antiviral activities of lectins (EC_{50} = 1–2 μg/ml; [6]). CV-N's oligosaccharide binding specificity is also unprecedented. In affinity chromatography experiments, CV-N is able to preferentially bind the oligomannose-8 (Man-8) and oligomannose-9 (Man-9) glycoforms of RNaseB and not the oligomannose-7 (Man-7), oligomannose-6 (Man-6), and oligomannose-5 (Man-5) glycoforms [7]. CV-N binds strongest to the larger high-mannose oligosaccharides, Man-8 [7] and Man-9 [8], and only these two oligomannoses exhibit significant inhibition of the CV-N-gp120 interaction [5] and interfere with CV-N's ability to block gp120-CD4 mediated fusion [8].

At present, no structural information is available for complexes between CV-N and high-mannose oligosaccharides, and the binding sites of only a very short mannoside (Man-α1→2-Man) [8, 9] have been mapped on CV-N. Although useful as an initial step in the analysis of the protein-sugar interaction, studies with short carbohydrate sequences cannot adequately address the observed tight binding of CV-N with either Man-8 or Man-9. In order to derive a more biologically relevant model, it is necessary to study the interaction of larger, branched mannosides with CV-N. Such studies are reported here. To circumvent problems due to aggregation and precipitation generally observed in interactions with high-mannose sugars such as Man-9 [8] and Man-8 [7], synthetic oligomannoside substructures of Man-9 were employed. Recent progress in solid-phase synthesis and solution-phase assembly [10] of oligosaccharides allows for the production of oligomannosides such as the branched nonamannoside *n*-pentyl glycoside, which lacks the chitobiose moiety at the reducing end of the oligosaccharide structure (Figure 1). Smaller substructures of the nonamannoside, the hexameric and trimeric cores, and the linear trimeric arm were also investigated.

The binding of this panel of oligomannosides (Figure 1) was initially assessed by nuclear magnetic resonance (NMR). Qualitative information from these studies was extended to a fully quantitative study of mannoside binding to CV-N by using the technique of isothermal titration calorimetry (ITC). We have previously used ITC to characterize the thermodynamics of CV-N binding to glycoproteins [7, 11] and to a single, purified oligosac-

[5]Correspondence: manuscripts@dtpax2.ncifcrf.gov (M.R.B.), gronenborn@nih.gov (A.M.G.)

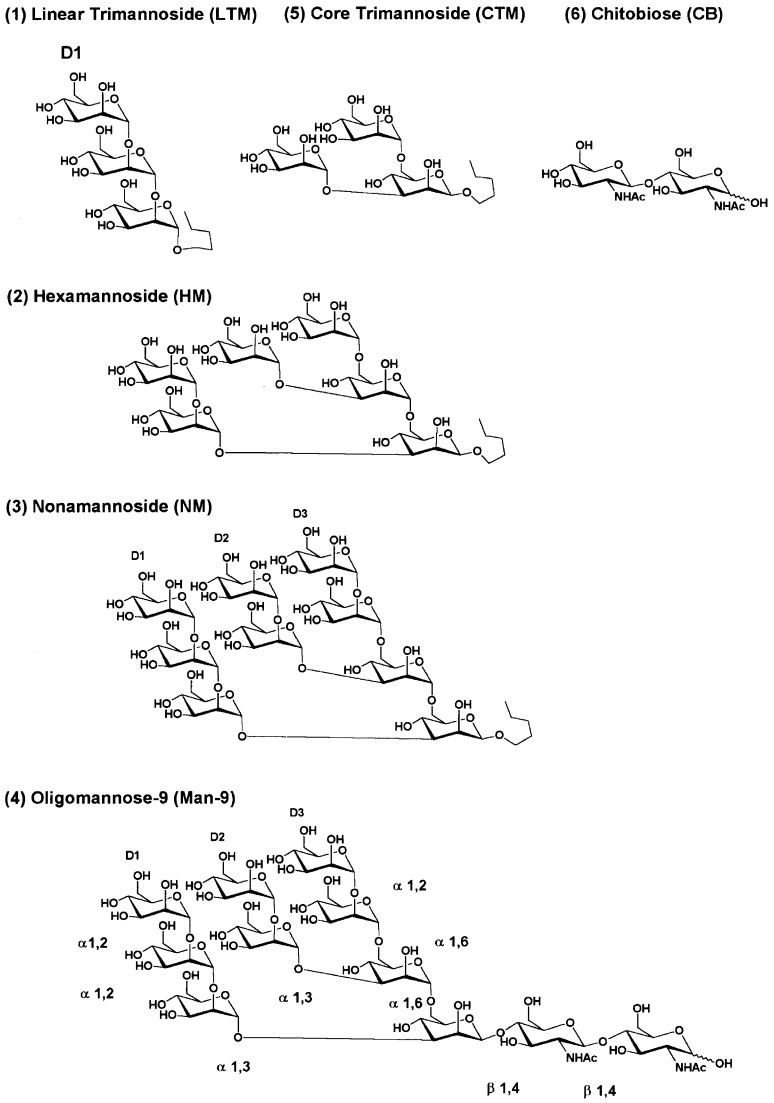

Figure 1. Chemical Structures and Names Assigned to the Various Mannosyl Substructures of Man-9

charide, oligomannose-8 (Man-8) [7]. ITC is the method of choice for determining the affinity of a ligand for a macromolecule and has been extensively employed in binding studies of mono-, di-, and other small, unbranched saccharides with their partner lectins [12, 13]. It is increasingly being applied to the study of branched oligosaccharides and their multivalent interactions with proteins [14, 15]. The combined data from our NMR and calorimetric titration studies allow us to propose a mechanism for the reported tight binding between CV-N and Man-9 and to provide clues toward understanding the unique biological activity of this protein.

Results and Discussion

NMR titration experiments with linear trimannoside (LTM), hexamannoside (HM), and nonamannoside (NM) indicated that binding of the three oligosaccharides to CV-N affects either one or two regions of the protein. These two regions on CV-N were essentially identical to the binding sites implicated in the CV-N binding of a dimannoside (Man-α1→2-Man) [9]. The interaction between CV-N and oligomannose-9 (Man-9) resulted in aggregation and precipitation and complete loss of NMR signal due to line broadening. Therefore, no structural information could be derived by NMR for this interaction. Binding was observed for all sugars except the core trimannoside (CTM) and chitobiose (CB).

Calorimetric titrations of LTM, HM, NM, and Man-9 with CV-N revealed that CV-N binding was largely driven by enthalpic contributions (negative ΔH values) as determined from the observed isotherms (Figure 2; Table 1). The larger sugars exhibited greater exothermic heats of binding (Figure 2). A negative ΔH of association suggested that favorable binding contacts such as polar/electrostatic, van der Waals, and hydrogen bonds were mediated between CV-N and these oligosaccharides. Binding was, however, entropically disfavored for all of the CV-N-oligosaccharide interactions (negative TΔS values; $\Delta G = \Delta H - T\Delta S$). This result indicated that the sum total of binding entropy due to solvation effects and to the rotational, translational, and conformational

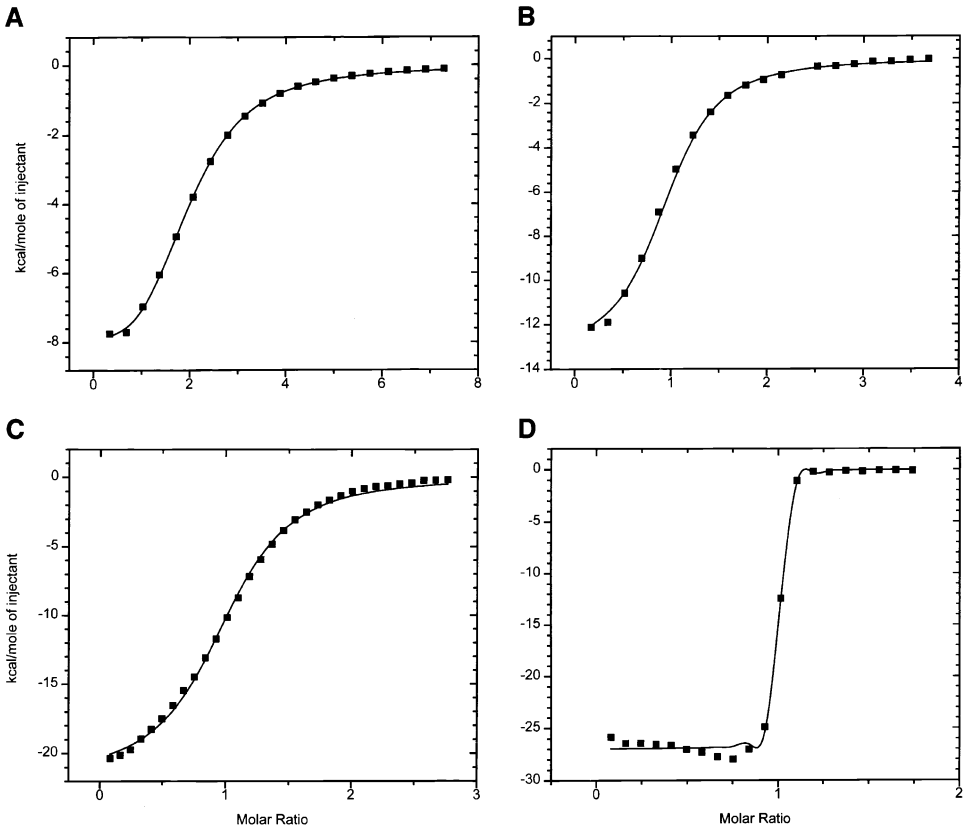

Figure 2. Calorimetric Titrations of CV-N

Calorimetric titrations of CV-N with (A) LTM, (B) HM, (C) NM, and (D) Man-9.
The solid lines represent fits to the data. The overall ΔH (kcal/mol) of binding and stoichiometry of the interaction is easily observed.

freedoms of CV-N and/or the oligosaccharides was greatly reduced as a result of binding. It is generally expected that complex formation reduces the translational, rotational, and, in some cases, the conformational entropies of the binding partners. If, however, binding is accompanied by expulsion of water from the binding interface, the gain in entropy of the water molecules would provide a favorable driving force for complex formation. Our results for the binding between CV-N and the high-mannose oligosaccharides suggest that the latter contributes minimally to the energetics of this interaction. An enthalpy-entropy compensation plot ($-\Delta H$ versus $-T\Delta S$; Figure 3A) showed a linear correlation ($r^2 = 0.98$). The observed slope of 1.23 demonstrated that the enthalpy and entropy terms were approximately equal in magnitude. However, the enthalpies of binding were favorable enough to offset the unfavorable binding entropies (Figure 3B), resulting in moderately tight binding interactions between the oligosaccharides and CV-N. Enthalpy-entropy compensation such as this is commonly observed for protein-oligosaccharide interactions [16].

Table 1. Overall Thermodynamic Parameters Recovered from the Binding Data of CV-N with Man-9 and with the Various Substructures of Man-9 Using a One-Site Model

	LTM	HM	NM	Man-9[2]
Enthalpy ΔH overall (kcal/mol)	−9.06 ± 0.10	−13.40 ± 0.16	−21.70 ± 0.22	−27.00 ± 0.18
Entropy TΔS overall (kcal/mol)	−2.67 ± 0.10	−5.66 ± 0.16	−13.97 ± 0.21	−16.17 ± 0.21
Free Energy ΔG overall[1] (kcal/mol)	−6.39 ± 0.03	−7.74 ± 0.04	−7.72 ± 0.03	−10.80 ± 0.21

CV-N titrations with CTM and CB resulted in basal levels of binding which could not be deconvoluted by the calorimetric software.
[1] $\Delta G = -RT\ln K_a$; T = 303 K.
[2] Precipitation observed.

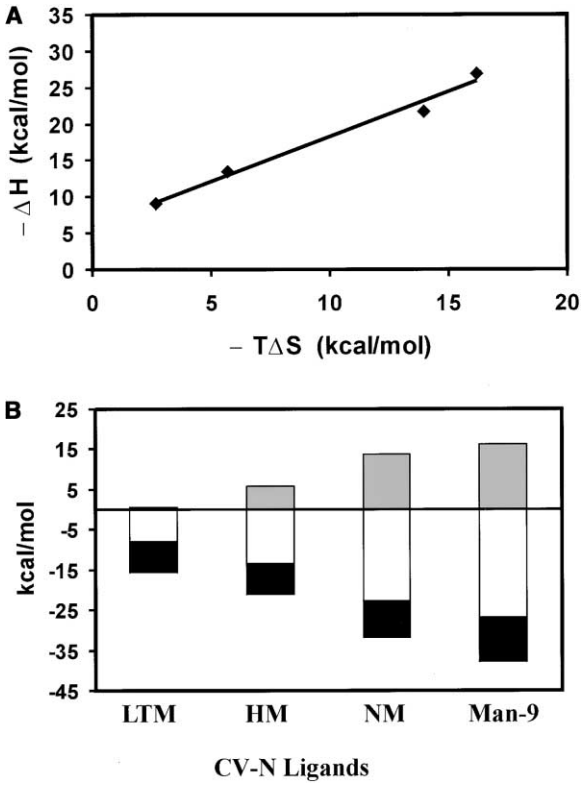

Figure 3. Enthalpy-Entropy Compensation

(A) Plot of $-\Delta H$ versus $-T\Delta S$ for the binding of CV-N to LTM, HM, NM, and Man-9. The solid line corresponds to fit of the data with a slope of 1.23.

(B) Dissection of the binding energetics ($\Delta G = \Delta H - T\Delta S$) of LTM, HM, NM, and Man-9 to CV-N. ΔG, black bars; $-T\Delta S$, gray bars; ΔH, white bars.

Binding of Core Trimannoside and Chitobiose to CV-N

Calorimetric titration experiments using core trimannoside and chitobiose with CV-N did not result in measurable affinities in the calorimetric experiments even at high concentrations of protein and sugar. The chitobiose disaccharide resides at the reducing end of an N-linked sugar via which the sugar is attached to the side chain amino group of asparagine in a given glycoprotein. This implies that the chitobiose is the least surface-exposed part of the sugar and in most cases will not be accessible for interaction. Similarly, CTM in high-mannose sugars is buried in the interior of the sugar structure and is thus less accessible. CV-N's inability to recognize CTM and CB was somewhat expected, since we had previously observed that complex oligosaccharides (which contain these same core structures) have no binding affinity to CV-N [7]. In this regard, it is interesting that chitobiose and core trimannose are specifically recognized by enzymes that cleave bi- and triantennary complex oligosaccharides but not by enzymes that process high-mannose oligosaccharides [17]. CV-N's lack of binding to CTM and CB suggested that its sugar binding properties might be similar to that of certain other high-mannose oligosaccharide binding proteins [17].

Binding of a Linear α-(1→2)Trimannoside to CV-N

CV-N's inability to recognize internal structures (CB and CTM) of Man-9 prompted us to examine other substructures of this oligosaccharide that may be responsible for binding CV-N. The linear trimannoside was synthesized and employed for structural and calorimetric studies. This sugar is composed of a unique string of three consecutive α1→2-linked mannoses that characterizes the D1 arm of Man-9.

Binding of LTM to CV-N was investigated by NMR. Chemical-shift mapping using ^{1}H-^{15}N HSQC spectroscopy revealed chemical-shift changes for 11 backbone amide resonances and 5 side chain amide resonances upon addition of one equivalent of sugar. For higher amounts of sugar, an additional 13 resonances were affected, exhibiting substantial line broadening. The changes observed were essentially identical to those reported for binding of a linear dimannoside (Manα1→2-Man) [9], and as will be discussed, the mapping of the two sugar-interacting sites on CV-N were similar in the cases of LTM and of a branched nonamannoside (Figures 4D and 4E).

Calorimetric analysis of the interaction between LTM and CV-N is consistent with a two-site binding model suggested by the structural data. The thermodynamic parameters for LTM binding at the two sites on CV-N were obtained by using a nonlinear least-squares fitting of the binding to either a one- or two-site model. The recovered thermodynamic parameters are summarized in Tables 1 and 2. For the two-site model, the enthalpies of LTM binding at site 1 and site 2 of CV-N were similar (ΔH_1 and $\Delta H_2 \simeq -8$ kcal/mol; Table 2), whereas the binding entropy at site 1 was more favorable ($T\Delta S_1 = -0.51$ kcal/mol versus $T\Delta S_2 = -2.75$ kcal/mol). The resulting equilibrium dissociation constant for binding of LTM at site 1 is a factor of 10 smaller than at site 2 ($K_{d1} = 3.48$ μM; $K_{d2} = 46.10$ μM), resulting in an overall 10-fold weaker binding of the sugar to site 2 on CV-N. This result was in agreement with the NMR titration data for LTM. The second sugar-interacting site on CV-N has been described as a semicircular cleft [9] which binds mannosides less efficiently than does the primary site. Our results with LTM are consistent with this finding.

Binding of Hexamannoside to CV-N

Extending the structure of linear LTM to hexamannoside represents the next logical step for a progressive synthesis toward larger oligomannose structures. The striking difference observed between the CV-N binding of CTM and LTM suggested that an extended binding epitope containing α1→2-linked mannoses may be a critical determinant for binding CV-N. We reasoned that if a core structure containing an α1→2-linked mannose terminus could be designed, then proper recognition by CV-N would be possible. HM represents the extended core region of Man-9 and, as such, is branched to a similar extent as is Man-9. It contains, however, only one of four terminal α1→2-linked mannoses of the larger oligosaccharide. The interaction of this hexamannoside with CV-N was again investigated by NMR. This constitutes the first structural study of CV-N with a branched oligosaccharide.

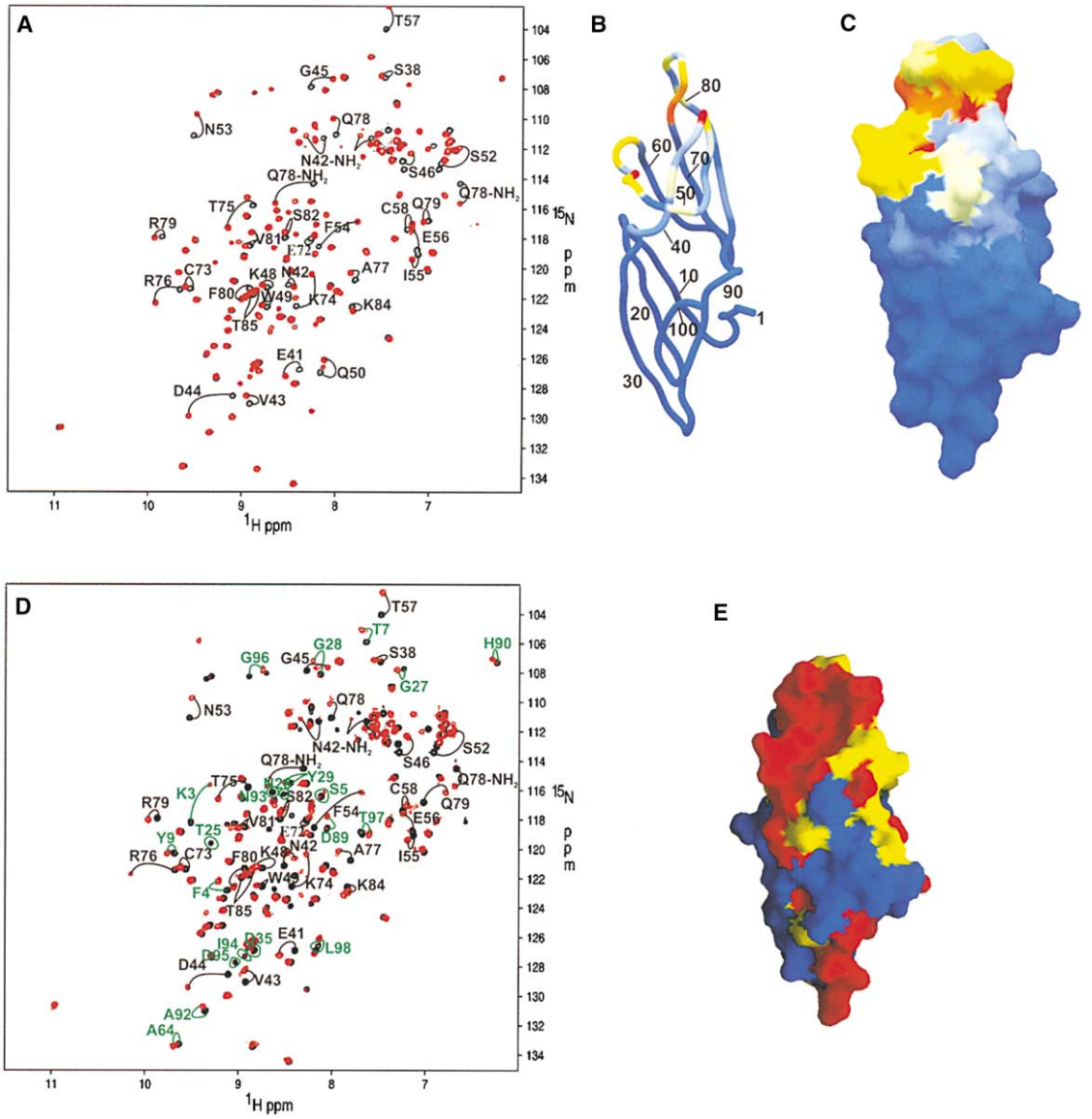

Figure 4. Structural Mapping of Sugar Binding Sites on CV-N

Superposition of the ^{1}H-^{15}N HSQC spectra of free CV-N and CV-N complexed with hexamannoside (A) and free CV-N and CV-N complexed with nonamannoside (D). Free protein (black) is at concentration of 100 μM, and the spectrum of the complexes (red) are shown at a hexamannoside/protein ratio of 15:1 and a nonamannoside/protein ratio of 7:1. Resonances are labeled by residue number and type with arrows connecting free (black) and complex (red) cross peaks. In (D), residues affected by binding of carbohydrate to the second site on the protein are labeled in green. Residues exhibiting intermediate exchange behavior on the chemical shift scale are circled. (B) shows a backbone tubular representation and (C) and (E) show molecular surface representations of the CV-N structure delineating the binding surfaces for the hexamannoside ([B] and [C]) or nonamannoside (E). The color coding in (B) and (C) reflects the normalized weighted average of the ^{1}H and ^{15}N chemical shifts calculated as $[\Delta\delta^2_{NH} + \Delta\delta^2_N/25)/2]^{1/2}\Delta_{max}$, where Δ_{max} is the maximum observed weighted shift difference (0.385 ppm for the amide cross peak of D44). The colors range from orange ($\Delta_{av}/\Delta_{max} = 1.0$) through yellow ($\Delta_{av}/\Delta_{max} = 0.5$) to blue ($\Delta_{av}/\Delta_{max} = 0$). In (E), residues not affected by nonomannose binding are colored blue, and those exhibiting small and large changes are yellow and red, respectively. Molecular structures were generated with the program GRASP [29], and the coordinates of CV-N employed are those of the solution NMR structure (Protein DataBank ID code 2EZN).

Similar to our findings with LTM, changes in amide resonances in the HSQC spectra of CV-N were observed. Indeed, identical resonances for which changes had occurred after addition of one equivalent of LTM were perturbed, indicating that the same region of the protein was involved in sugar binding (Figures 4A–4C). Unexpectedly, however, even a 19-fold molar excess of HM did not result in further changes in the spectrum. This suggests that the hexamannoside lacks the structural features necessary for detectable binding to both sites on the protein. Alternatively, the hexamannoside may represent a more conformationally restricted molecule than LTM, hindering the necessary conformational change for binding to the second site on the protein.

Table 2. Thermodynamic Parameters Recovered from the Binding Data for LTM, HM, and NM to CV-N Using a One-Site Model for HM and a Two-Site Model for LTM and NM

	LTM	HM	NM
Stoichiometry			
sugar:CV-N	2:1	1:1	$(1:1)_2$
Enthalpy			
ΔH_1			
(kcal/mol)	−8.07 ± 0.10	−13.40 ± 0.16	−22.80 ± 0.25
ΔH_2			
(kcal/mol)	−8.76 ± 0.14		−0.38 ± 0.26
Entropy			
$T\Delta S_1$			
(kcal/mol)	−0.51 ± 0.13	−5.66 ± 0.16	−13.71 ± 0.25
$T\Delta S_2$			
(kcal/mol)	−2.75 ± 0.10		7.33 ± 0.26
Free Energy			
$^1\Delta G_1$			
(kcal/mol)	−7.56 ± 0.13	−7.74 ± 0.04	−9.09 ± 0.10
$^1\Delta G_2$			
(kcal/mol)	−6.01 ± 0.02		−7.72 ± 0.09
Affinity			
Kd_1			
(μM)	3.48 ± 0.78	2.61 ± 0.19	0.27 ± 0.05
Kd_2			
(μM)	46.10 ± 1.70		2.70 ± 0.42

$^1\Delta G = -RTlnK_a$; T = 303 K.

Future structural studies of the complex between CV-N and HM may shed some light on these issues.

Calorimetric titration data revealed that HM binds with moderate affinity to CV-N (Table 2). The analysis of the binding isotherm (Figure 2B) yielded a ΔG value of −7.74 kcal/mol, and the data could be fitted well to a one-site model. The recovered parameters showed that the HM-CV-N interaction was enthalpically driven ($\Delta H_1 = -13.40$ kcal/mol). Interestingly, the binding enthalpy for HM is more favorable than that for LTM ($\Delta\Delta H_1 = -5.33$ kcal/mol), although both sugars appeared to structurally affect site 1 on CV-N in a similar manner. This gain in binding enthalpy was, however, almost completely compensated by the loss in favorable binding entropy, resulting in an equilibrium dissociation constant ($K_{d1} = 2.61 \pm 0.19$ μM) that was comparable to that of LTM ($K_{d1} = 3.48 \pm 0.78$ μM). This suggested that CV-N can recognize and bind with similar affinity to an α1→2-linked mannose in a sterically unhindered structure (LTM) as well as to one contained within a core high-mannose oligosaccharide (HM). Since no binding of CTM ([α-Man-(1→3)][α-Man-(1→6)]-α-Man) to CV-N was observed, it seemed unlikely that this substructure(s) in HM could have mediated interaction with CV-N.

Binding of Nonamannoside to CV-N

The closest structural similarity between any of our present oligosaccharides and Man-9 exists for the nonamannoside. In contrast to Man-9, no aggregation and/or precipitation of CV-N upon sugar binding occurred, rendering this molecule an ideal analog for structural and thermodynamic investigations. Aggregation and precipitation had been reported for Man-9's interaction with CV-N [8], and it is well known that nonequilibrium conditions prevent the extraction of correct thermodynamic data. NM lacks the chitobiose moiety of Man-9 but retains the rest of Man-9's internal branched construction and, more importantly, the three mannosyl arms of the oligosaccharide. Using NM it was possible to monitor the sugar binding by NMR, thereby allowing for the first time a study of a biologically relevant CV-N-high-mannose interaction. As with LTM, two sites on CV-N were affected by binding. Superimpositions of the free and NM-bound HSQC spectra of CV-N are displayed in Figure 4D, and identical regions on the three-dimensional protein structure as previously observed for LTM are mapped as interaction sites (Figure 4E). These results suggest that the major structural determinants on high-mannose sugars responsible for high affinity CV-N binding contain α1→2 linked mannoses.

Calorimetric titration of CV-N with NM was performed and compared to the LTM-CV-N interaction (Figure 2C). Since two sites on the protein were identified by NMR, the experimental binding isotherm was fitted to a two-site model (Table 2). Similar to LTM, a 10-fold difference in sugar binding affinity was observed between the two sites on CV-N ($K_{d1} = 0.27$ μM versus $K_{d2} = 2.70$ μM). However, comparing the absolute values of NM's binding affinities with those of LTM ($K_{d1} = 3.48$ μM, $K_{d2} = 46.10$ μM), a ~15-fold difference between the respective affinities was noted. Given the NMR results, we attribute the observed binding affinity between NM and CV-N to multivalent binding.

Another significant difference between NM and LTM was noted in the binding energetics. Comparing the thermodynamic parameters using the two-site model, binding of NM to site 1 appeared to be largely driven by enthalpic contributions, whereas entropy alone (positive ΔS_1 value) was responsible for binding to site 2. In contrast, for LTM, enthalpy favored binding to both sites.

A negative ΔH of association is generally believed to be due to favorable binding contacts, such as polar/electrostatic, van der Waals, and hydrogen bonds, between a ligand and a macromolecule. A positive ΔS, on the other hand, is more difficult to interpret. It could be due to several binding modes for NM at the site 2 on CV-N. Alternatively, flexibility of the protein and/or sugar in the complex and solvation effects may also have contributed to the observed positive entropy of binding.

Many naturally occurring oligosaccharides and glycoconjugates are multivalent, thereby increasing the apparent affinity for lectins relative to monovalent analogs [18]. Multivalency for the NM-CV-N interaction thus seemed a plausible mechanism. The three "arms" of NM each contain α1→2-linked mannoses, allowing a single molecule of NM to interact with more than one molecule of CV-N. An experimental test of this hypothesis is easily possible. NMR relaxation measurements allow an estimation of the molecular mass of the molecule or complex under investigation. We measured heteronuclear T_2 values for the amide protons and amide nitrogens in the different complexes described here. For uncomplexed CV-N and complexes between CV-N and LTM or HM, average T_2 values of $\sim$50 ms and $\sim$110 ms were observed for protons and nitrogens, respectively, consistent with one protein molecule per complex. For the complex between CV-N and NM, average T_2 values of $\sim$21 ms and $\sim$64 ms were obtained, significantly shorter than expected for a 1:1 complex. Indeed, these values are similar to those measured for a domain-swapped dimer structure of CV-N, previously characterized by NMR [19], suggesting a species significantly larger than a single CV-N protein bound to either one or two sugar molecules. In order to further assess the oligomerization state of the sugar-CV-N complexes, we carried out sedimentation studies by analytical ultracentrifugation. Results indicated that the NM-CV-N complex was polydisperse, predominantly containing species of $\sim$22–24 kDa size. We therefore concluded that the NM-CV-N complex contains at least two protein molecules.

Closer examination of the NM-CV-N calorimetric experiment revealed additional support for the involvement of multivalent interactions. Comparison of the overall binding enthalpies observed for LTM and NM upon interaction with CV-N (Figures 2A and 2C) revealed that the ΔH value for NM was approximately twice that of LTM. On the other hand, the binding entropies did not scale accordingly. Instead, $T\Delta S$ was much more negative ($-$13.97 kcal/mol) than twice the $T\Delta S$ value of $-$2.67 kcal/mol for LTM. This finding suggested that NM is a multivalent ligand that binds to separate macromolecules [18]. An analogous behavior has been reported for the interaction of concanavalin A with multivalent sugars [14]. The ability of NM to crosslink two CV-N molecules and for CV-N to bind two NMs at site 1 and site 2 suggests that the 1:1 stoichiometry observed in the calorimetric experiment results from two protein molecules interacting with two sugar molecules. This is in agreement with the sedimentation studies described above. Similar 2:2 (1:1) stoichiometries have been described for interactions between bivalent lectins and bivalent oligosaccharide ligands [20, 21]. A proposed binding scheme illustrating the possible species and their equilibria is provided in Figure 5.

Binding of Man-9 to CV-N

Despite several attempts to elucidate the structural features of Man-9 binding to CV-N by NMR, complex formation was accompanied by extreme line broadening and ultimately resulted in precipitation. Similar problems were encountered in the titration calorimetric experiment. It therefore was impossible to extract an accurate value for binding affinity from such an isotherm (Figure 2D). If we treated the binding as an equilibrium isotherm, a meaningless value was obtained. However, an accurate estimation of the binding enthalpy (ΔH overall) was possible, as this parameter could be extrapolated from the isotherm well before the point of aggregation, at the beginning stages of the titration experiment. The ΔH of binding ($-$27 kcal/mol) was very similar to that observed for NM (Figure 2C), albeit slightly more negative. Binding of Man-9 to CV-N appeared to also involve multisite interactions similar to those between CV-N and NM. The calculated difference in ΔH values for the CV-N interaction with Man-9 and LTM was large ($\Delta\Delta H = -17.94$ kcal/mol; Figures 2A and 2D; Table 1), suggesting that Man-9 bound more than one CV-N molecule. An exact molecular weight of the protein-oligosaccharide complex was, however, impossible to determine by analytical ultracentrifugation due to the precipitation. This implies a substantial size for the complex.

Precipitation of Man-9-CV-N occurred at about a 1:1 molar ratio (Figure 2D). This suggested that prior to precipitating, the Man-9-CV-N association was similar to that of the NM-CV-N complex. Sedimentation results had indicated that although multimerization of the NM-CV-N complex had been possible, formation of higher-order structures was not greatly favored under our present equilibrium conditions. The NM binding affinities for site 1 and site 2 on CV-N were not high enough to drive the formation of very large, insoluble oligosaccharide-protein complexes. This is different for Man-9 binding, where higher binding affinities at site 1 and 2 could easily promote the formation of higher aggregates.

Taking all of the above results together yields the following picture. The chitobiose unit (GlcNAc-β1→4-GlcNAc) that is present in Man-9 but absent in NM appears to contribute to the observed tight binding between Man-9 and CV-N, although CB by itself had no affinity for CV-N (Table 1). This suggested that its presence in the Man-9 structure enhanced the ability of the α1→2-linked mannoses to mediate tight, multivalent interactions with CV-N. Molecular dynamics simulations of high-mannose oligosaccharides previously indicated that the D1 and D3 arms are more solvent exposed than the D2 arm, with the D2 arm being held closer to the chitobiose core region [22]. In addition, biochemical data have revealed that the terminal mannose on D2 is protected from cleavage through its interactions with chitobiose [23] and that the rate of cleavage by mannosidases increases upon removal of the reducing GlcNAc [24]. It therefore is possible that the CB unit in Man-9 may help to retract the D2 arm closer to the core region, creating less steric hindrance for the D1 and D3 arms,

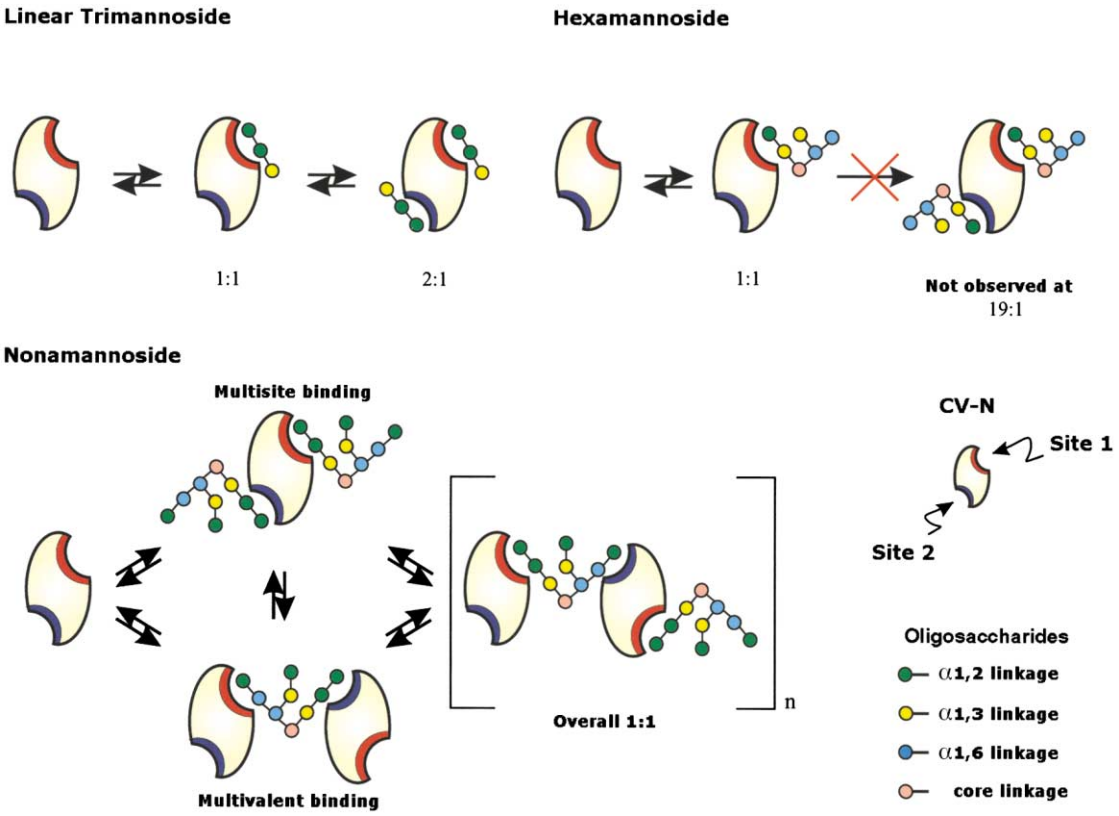

Figure 5. Schematic Depiction of LTM, HM, and NM Binding to CV-N

CV-N is represented by an ellipsoid and both binding sites are marked. Site 1 is colored blue and site 2 red. The individual sugar units on the oligosaccharides responsible for interacting with CV-N are color coded according to their linkage pattern.

allowing these arms to optimally extend into CV-N's sugar binding sites. This line of reasoning is fully supported by the ITC data. Binding of Man-9 to CV-N resulted in a more favorable enthalpy than the binding of NM ($\Delta\Delta H = -5.3$ kcal/mol; Figures 2C and 2D; Table 1), suggesting that Man-9 can engage in more intimate contacts with CV-N. A stronger binding by Man-9 at both site 1 and site 2 on CV-N will fix the higher-order structures that are formed during the course of multivalent, multisite binding between the oligosaccharide and the protein (Figure 5) and result in precipitation of these complexes.

Significance

The interaction between the antiviral protein, cyanovirin-N (CV-N), and high-mannose oligosaccharides of viral glycoproteins has been difficult to map due to severe aggregation of the protein-sugar complexes. Recent progress in solid-phase synthesis and solution-phase assembly [10] of oligosaccharides has allowed the production of a series of linear and branched oligomannosides employed in the present work to investigate these interactions in greater detail. Using NMR and isothermal titration calorimetry, the multivalent binding of branched oligomannosides to CV-N was dissected using synthetic substructures of Man-9. We demonstrated that CV-N specifically recognizes the α1→2-linked mannosyl-containing arms of Man-9 but does not bind the oligosaccharide's internal core regions such as the trimannose core or the chitobiose. Both the nonamannoside and the trimannosyl D1 arm bind CV-N in essentially identical fashion at two distinct protein sites. The size of the CV-N-nonamannoside complex indicates that on average two molecules of CV-N are linked via the oligosaccharide. This linking, together with the fact that CV-N binds two Man-9 analog molecules, is most likely responsible for the tight association between CV-N and this oligosaccharide. Characterization of the multisite, multivalent interaction between CV-N and high-mannose oligosaccharides sheds light on the biological activity of CV-N. The mechanism for the practically irreversible association of CV-N with high-mannose oligosaccharides brought about by these unique molecular interactions is outlined in the present paper. We suggest that the potent HIV-inactivating activity of CV-N is in large part due to its ability to block viral-cell fusion by irreversibly binding and linking oligosaccharides on gp120 and gp41, thereby crosslinking discrete areas in these proteins and rendering them incapable to undergo the

necessary conformational changes for interaction with host-cell receptors.

Experimental Procedures

Source of Cyanovirin-N and Oligosaccharide Ligands

CV-N

Uniformly ^{15}N-labeled CV-N used for both NMR and ITC titrations was purified as described in Barrientos et al. [25]. The wild-type variant used in the present study comprises five additional N-terminal amino acids (GSHMG) and exhibited both anti-HIV activity and gp120 binding, essentially indistinguishable from the original 101-amino-acid-containing protein.

Chitobiose and Man-9

N, N′-diacetylchitobiose was purchased from Sigma. Oligomannose-9 (Man-9) was purchased from Glyko, Inc.

Synthesis of Branched High-Mannose Oligosaccharides

Solution-phase synthesis of the pentyl core trimannoside, hexamannoside, and nonamannoside (Figure 1) has been described previously [10]. The linear trimannoside was prepared using an automated solid-phase oligosaccharide synthesizer as described previously [26, 27].

Quantitation of CV-N and Oligosaccharides

^{15}N-CV-N concentration was quantified using a Hitachi model L8800 amino acid analyzer according to manufacturer's protocols. The concentrations of the synthetic oligosaccharides and Man-9 were determined by compositional analysis performed by the Complex Carbohydrate Research Center at the University of Georgia.

NMR Titration Experiments

Samples contained 100 μM CV-N in 20 mM sodium phosphate buffer (pH 6.0), 0.05% NaN_3, 90% H_2O/10% D_2O. ^1H-^{15}N HSQC spectra were recorded at 25°C on Bruker DRX600 and DMX750 spectrometers equipped with triple-gradient triple-resonance probes. All data were processed and analyzed with the NMRPipe suite of programs [28]. Titrations were performed by adding small aliquots from stock solutions of 3.0 mM hexamannose and 4.2 mM nonamannose.

Isothermal Titration Calorimetry Experiments

The calorimetric titrations were performed on a MCS-ITC titration calorimeter from Microcal, Inc. (Northampton, MA). In a typical experiment, 10 μl aliquots of an oligosaccharide solution were injected from a 250 μl syringe into a rapidly mixing (400 rpm) solution of CV-N (cell volume = 1.3472 ml). Control experiments involved injecting identical amounts of the oligosaccharide solution into buffer without CV-N. The concentrations of CV-N were 0.035–0.076 mM, and those of the sugars were 0.48–2.89 mM. Titrations were carried out at 30°C in 50 mM sodium phosphate buffer, 0.2 M NaCl, 0.02% NaN_3 (pH 7.5). The isotherms, corrected for dilution/buffer effects, were fit using the Origin ITC Analysis software according to manufacturer's protocols. A nonlinear least-square method was used to fit the titration data and to calculate the errors. From the binding curve, values for enthalpy, stoichiometry, and binding affinity were extracted. Thermodynamic parameters were calculated using $\Delta G = -RT\ln K_a$, $\Delta G = \Delta H - T\Delta S$.

Acknowledgments

We thank Dr. Kirk Gustafson for valuable advice and for critical reading of the manuscript, Ray Sowder of SAIC-Frederick for amino acid analysis of proteins, John Louis for protein purification, Rodolpho Ghirlando for analytical ultracentrifugation, and James McMahon for invaluable help with the figures. This work was supported by an NIH Biotechnology Training Grant (D.M.R.), GlaxoSmithKline (Research Scholar Award to P.H.S.), the Alfred P. Sloan Foundation (Scholar Award to P.H.S.), and the Intramural AIDS Targeted Antiviral Program of the Office of the Director of the National Institutes of Health (A.M.G.).

Received: May 17, 2002
Revised: September 9, 2002
Accepted: September 9, 2002

References

1. Geyer, H., Holschback, C., Hunsmann, G., and Schneider, J. (1988). Carbohydrates of human immunodeficiency virus: structures of oligosaccharides linked to the envelope glycoprotein gp120. J. Biol. Chem. *263*, 11760–11767.
2. Yeh, J., Seals, J.R., Murphy, C.I., van Halbeek, J., and Cummings, R.D. (1993). Site-specific N-glycosylation and oligosaccharide structures of recombinant HIV-1 gp120 derived from a bacculovirus expression system. Biochemistry *32*, 11087–11099.
3. Losman, B., Bolmstedt, A., Schonning, K., Bjorndal, A., Westin, C., Fenyo, E.M., and Olofsson, S. (2001). Protection of neutralization epitopes in the V3 loop of oligomeric human immunodeficiency virus type I glycoprotein 120 by N-linked oligosaccharides in the V1 region. AIDS Res. Hum. Retroviruses *17*, 1067–1076.
4. Boyd, M.R., Gustafson, K.R., McMahon, J.B., Shoemaker, R.H., O'Keefe, B.R., Mori, T., Gulakowski, R.J., Wu, L., Rivera, M.I., Laurencot, C.M., et al. (1997). Discovery of cyanovirin-N, a novel human immunodeficiency virus-inactivating protein that binds viral surface envelope glycoprotein gp120: potential applications to microbicide development. Antimicrob. Agents Chemother. *41*, 1521–1530.
5. Bolmstedt, A.J., O'Keefe, B.R., Shenoy, S.R., McMahon, J.B., and Boyd, M.R. (2001). Cyanovirin-N defines a new class of antiviral agent targeting N-linked, high-mannose glycans in an oligosaccharide-specific manner. Mol. Pharmacol. *59*, 949–954.
6. Charan, R.D., Munro, M.H., O'Keefe, B.R., Sowder, R.C., II, McKee, T.C., Currens, M.J., Pannell, L.K., and Boyd, M.R. (2000). Isolation and characterization of Myrianthus holstii lectin, a potent HIV-1 inhibitory protein from the plant Myrianthus holstii (1). J. Nat. Prod. *63*, 1170–1174.
7. Shenoy, S.R., O'Keefe, B.R., Bolmstedt, A.J., Cartner, L.K., and Boyd, M.R. (2001). Selective interactions of the human immunodeficiency virus-inactivating protein cyanovirin-N with high-mannose oligosaccharides on gp120 and other glycoproteins. J. Pharmacol. Exp. Ther. *297*, 704–710.
8. Bewley, C.A., and Otero-Quintero, S. (2001). The potent anti-HIV protein cyanovirin-N contains two novel carbohydrate binding sites that selectively bind to Man(8) D1D3 and Man(9) with nanomolar affinity: implications for binding to the HIV envelope protein gp120. J. Am. Chem. Soc. *123*, 3892–3902.
9. Bewley, C.A. (2001). Solution structure of a cyanovirin-N:Man alpha 1–2Man complex: structural basis for high-affinity carbohydrate-mediated binding of gp120. Structure *9*, 931–940.
10. Ratner, D.M., Plante, O.J., and Seeberger, P.H. (2002). A linear synthesis of branched high-mannose oligosaccharides from the HIV-1 viral surface glycoprotein gp120. Eur. J. Org. Chem. *5*, 826–833.
11. O'Keefe, B.R., Shenoy, S.R., Xie, D., Zhang, W., Muschik, J.M., Currens, M.J., Chaiken, I., and Boyd, M.R. (2000). Analysis of the interaction between the HIV-inactivating protein cyanovirin-N and soluble forms of the envelope glycoproteins gp120 and gp41. Mol. Pharmacol. *58*, 982–992.
12. Bachhawat-Sikder, K., Thomas, C.J., and Surolia, A. (2001). Thermodynamic analysis of the binding of galactose and poly-N-acetyllactosamine derivatives to human galectin-3. FEBS Lett. *500*, 75–79.
13. Surolia, A., Sharon, N., and Schwarz, F.P. (1996). Thermodynamics of monosaccharide and disaccharide binding to Erythrina corallodendron lectin. J. Biol. Chem. *271*, 17697–17703.
14. Dam, T.K., Roy, R., Das, S.K., Oscarson, S., and Brewer, C.F. (2000). Binding of multivalent carbohydrates to concanavalin A and Dioclea grandiflora lectin. Thermodynamic analysis of the "multivalent effect." J. Biol. Chem. *275*, 14223–14230.
15. Asensio, J.L., Canada, F.J., Siebert, H.C., Laynez, J., Poveda, A., Nieto, P.M., Soedjanaamadja, U.M., Gabius, H.J., and Jimenez-Barbero, J. (2000). Structural basis for chitin recognition by

defense proteins: GlcNAc residues are bound in a multivalent fashion by extended binding sites in hevein domains. Chem. Biol. *7*, 529–543.

16. Chervenak, M.C., and Toone, E.J. (1995). Calorimetric analysis of the binding of lectins with overlapping carbohydrate-binding ligand specificities. Biochemistry *34*, 5685–5695.
17. Waddling, C.A., Plummer, T.H., Tarentino, A.L., and Van Roey, P. (2000). Structural basis for the substrate specificity of endo-beta-N-acetylglucosamininidase F(3). Biochemistry *39*, 7878–7885.
18. Dam, T.K., Roy, R., Page, D., and Brewer, C.F. (2002). Negative cooperativity associated with binding of multivalent carbohydrates to lectins. Thermodynamic analysis of the "multivalent effect." Biochemistry *41*, 1351–1358.
19. Barrientos, L.G., Louis, J.M., Botos, I., Mori, T., Han, Z., O'Keefe, B.R., Boyd, M.R., Wlodawer, A., and Gronenborn, A.M. (2002). The domain-swapped dimer of Cyanovirin-N is in a metastable folded state. Reconciliation of X-ray and NMR structures. Structure *10*, 1–20.
20. Ambrosino, R., Barone, G., Castronuovo, G., Ceccarini, C., Cultrera, O., and Elia, Y. (1987). Protein-lignd interaction. A calorimetric study of the interaction of oligosaccharides and hen ovalbumin glycopeptides with concanavalin A. Biochemistry *26*, 3971–3975.
21. Swaminathan, C.P., Gupta, D., Sharma, V., and Surolia, A. (1997). Effect of substituents on the thermodynamics of D-galactopyranoside binding to winged bean (Psophocarpus tetragonologbus) basic lectin. Biochemistry *36*, 13428–13434.
22. Balaji, P.V., Qasba, P.K., and Rao, V.S. (1994). Molecular dynamics simulations of high-mannose oligosaccharides. Glycobiology *4*, 497–515.
23. Schweden, J., and Bause, E. (1989). Characterization of trimming Man-9-mannosides from pig liver. Purification of a catalytically active fragment and evidence for the transmemembrane nature of the intact 65 kDa enzyme. Biochem. J. *264*, 347–355.
24. Bause, E., Breuer, W., Schweden, J., Roeser, R., and Geyer, R. (1992). Effect of substrate structure on the activity of Man-9-mannosidase from pig liver involved in N-linked oligosaccharide processing. Eur. J. Biochem. *208*, 451–457.
25. Barrientos, L.G., Louis, J.M., Hung, J., Smith, T.H., O'Keefe, B.R., Gardella, R.S., Mori, T., Boyd, M.R., and Gronenborn, A.M. (2002). Design and initial characterization of a circular permuted variant of the potent HIV-inactivating protein Cyanovirin-N. Proteins *46*, 153–160.
26. Plante, O.J., Palmacci, E.R., and Seeberger, P.H. (2001). Automated solid-phase synthesis of oligosaccharides. Science *291*, 1523–1527.
27. Andrade, R.B., Plante, O.J., Melean, L.G., and Seeberger, P.H. (1999). Solid-phase oligosaccharide synthesis: preparation of complex structures using a novel linker and different glycosylating agents. Org. Lett. *1*, 1811–1814.
28. Delaglio, F., Grzesiek, S., Vuister, G.W., Zhu, G., Pfeifer, J., and Bax, A. (1995). NMRPipe: a multidimensional spectral processing system based on UNIX pipes. J. Biomol. NMR *6*, 277–293.
29. Nicholls, A., Sharp, K.A., and Jonig, B. (1991). Protein folding and association: insights from the interfacial and thermodynamic properties of hydrocarbons. Proteins *11*, 281–296.